

Gas-Well Deliverability Monitoring: Case Histories

T.S. Thrasher, SPE, Phillips Petroleum Co.

26181

Summary

This paper presents practical techniques that can be used to monitor gas-well performance. These techniques, along with the routine examination of performance data, can help the engineer maintain production potential and extend well life. This paper demonstrates the importance of monitoring well performance on a regular basis through case history examples. Four types of well conditions are described: (1) deterioration in performance over time, (2) drainage area change, (3) liquid loading, and (4) tubing design constraint. This paper also discusses the use of a personal computer program as a tool to facilitate and encourage gas-well performance monitoring.

Introduction

Gas-well performance monitoring involves simple methods and techniques for data preparation and analysis. Case histories using field data show how these procedures enhance available data and justify monitoring efforts. The examples illustrate how monitoring production performance has helped identify wells where deliverability has deteriorated or reserves diminished. Even the most prudent engineer using conventional and advanced decline-curve analysis methods can overlook deterioration in well performance over a long period.

By plotting spot gas rate and flowing wellhead-pressure measurements directly on the backpressure curve, we can flag changes in deliverability immediately. We can help flag changes in the material-balance relationship (reserves) by taking advantage of shut-ins to obtain static wellhead pressure. These measurements can be obtained without conducting expensive special tests, which result in production interruption.

Today's total-flow meters and surface electronic pressure instrumentation are excellent sources for obtaining quality performance data.

The role of the interdisciplinary team and its impact on achieving well-performance objectives is identified and highlighted by field examples. A brief review of the governing flow equations is presented along with a method to display the minimum lift-gas rate directly on the backpressure plot.

Statement of Theory

Pioneers¹⁻⁴ in the field of gas technology have studied the production characteristics of gas wells by using observed performance data. They have documented simple but reasonably accurate equations that describe the relationship between gas rate and pressure drawdown. Rawlins and Schellhardt¹ developed the empirical relationship to describe their observation of hundreds of multirate gas-well tests:

$$q_{sc} = C(p_r^2 - p_{wf}^2)^n \quad (1)$$

This relationship forms the basis of the log-log backpressure curve. The backpressure plot normally is constructed with gas rate on the x axis vs. the difference in reservoir pressure, p_r , squared and flowing bottomhole pressure, p_{wf} , squared. The appropriate pressure function (pressure, pressure squared, or pseudopressure⁵) can replace pressure squared depending on the magnitude and range of pressure variation. Points that correspond to the same flow time

(transient flow) or stabilized (pseudosteady-state flow) are plotted. A similar form of Eq. 1—which refers to surface flow conditions and includes the affects of tubing, downhole chokes, and other friction loss plus slippage—is the wellhead backpressure equation:

$$q_{sc} = C(p_e^2 - p_i^2)^n \quad (2)$$

Points from a multipoint test form a line with an inverse slope, n , and coefficient C . Industry usage refers to n as the slope of the curve. The value of n ranges from 0.5 to 1.0. Single-layer reservoir performance with no high-velocity flow component should exhibit n values equal to one. High-velocity flow is a rate-dependent positive-skin effect that reduces the bottomhole flow potential and causes the n value to deviate from one. Multilayer reservoir performance with no crossflow and no high-velocity flow can exhibit n values of less than one.

Muskat⁶ discusses several models that modify Darcy's law to handle high-velocity flow in the reservoir. Forchheimer⁷ expresses this relationship as

$$dp/dr = av + bv^2 \quad (3)$$

Green and Duwaz⁸ and Cornell and Katz⁴ express Eq. 3 in terms of fluid and rock properties:

$$dp/dr = (\mu/k)v + \beta\rho v^2 \quad (4)$$

The high-velocity coefficient, β , in Eq. 4 is a property of the formation rock that accounts for the deviation from Darcy's law. A useful form of Eq. 4 in oilfield units for transient gas flow in terms of pressure squared is

$$(p_i^2 - p_w^2) = \frac{1,424(\bar{\mu}\bar{z})T}{kh} \{ (0.5[Ln(t_D) + 0.809] + S)q_{sc} + Dq_{sc}^2 \} \quad (5)$$

where

$$t_D = \frac{0.0002637kt}{\phi\mu_i c_{ri} r_w^2} \quad \text{and} \quad D = \frac{2.226 - 10^{-6}\beta k h y_g}{h\rho r_w \mu_i}$$

A useful form of Eq. 4 in oilfield units for transient gas flow in terms of pseudo-pressure can be expressed by

$$\left[m(p_i) - m(p_{wf}) \right] = \frac{1,424T}{kh} \{ (0.5[Ln(t_D) + 0.809] + S)q_{sc} + Dq_{sc}^2 \} \quad (6)$$

Experience has shown that performance characteristics are easily identified by studying the log-log backpressure curve.^{9,10} A standard format for the backpressure curve is achieved by using 3 × 3 cycle log-log graph paper or the equivalent computer-generated plot with square grids. Plotting in this format is not to be confused with the gas IPR^{11,12} curve and plotting method, which normally is a Cartesian plot used for system analysis.

Liquid Loading

We can enhance monitoring efforts by plotting the minimum lift rate directly on the conventional backpressure plot. This effort can help identify wells that are loaded up with liquid (water or oil condensate) production. The technique can also help flag wells that are approaching rates that can result in well liquid loading.¹³ By plotting the erosional rate directly on the backpressure plot, we can flag production that is too high for current tubing size and wellhead operat-

ing conditions. Excessively high rates can enhance corrosion and erosional forces¹⁴ as discussed in API RP 14E.

Turner *et al.*¹⁵ propose physical models for the removal of liquid from gas wells. We can calculate a minimum rate from Eq. 7 as a function of terminal velocity of the liquid particle, v_t , pressure, p , cross-sectional area of the tubing or casing, A , and temperature, T .

$$q_c = 3.06pv_t A/Tz \dots\dots\dots (7)$$

Terminal velocity is calculated as a function of the difference between fluid and gas density, ρ , and interfacial tension, σ :

$$v_t = 1.593 \left[\frac{\sigma^{3/4} (\rho_L - \rho_g)}{\rho_g^{1/4}} \right] \dots\dots\dots (8)$$

Eq. 8 does not include the 20% safety factor added by Turner. It is common practice to use the wellhead flowing pressure and cross-sectional area of the top tubing string to calculate the minimum rate. Pressure/temperature conditions and tubing configurations have been encountered where this practice would calculate lift rates that were too low. These situations pertain to cases where production tubing is set considerably above the perforations in the casing, a larger tubing size is set downhole, or downhole pressure and temperature conditions require a higher lift rate. In such cases, the calculations must be performed at both downhole and wellhead conditions.¹⁶ Coleman *et al.*¹⁷ recently verified Turner *et al.*'s relationship using data collected from 17 field tests and present an excellent review of this topic. It should be noted that Coleman *et al.*'s work focuses on wells that have wellhead pressures in the 800- to 1,000-psi range, while Turner *et al.*'s work involves wells with wellhead pressures greater than 1,000 psi. Bizanti¹³ presents pressure/temperature/diameter relationships.

This paper proposes plotting the minimum lift-gas rate directly on the backpressure plot as a function of pressure. In cases where the surface-tubing configuration is used, the minimum lift-rate values from initial shut-in to atmospheric pressure are determined in 50-psi increments. Where a downhole calculation is required, the values of minimum lift rate are determined from initial reservoir pressure to a minimum flowing pressure. These values are displayed on the bottomhole curve. Alternatively, the minimum lift-gas rate under current producing conditions can be determined and displayed as a vertical line on the backpressure plot. This calculation can be for a single location (wellhead) or at various points, depending on the flow-string configuration.

An overlay of the minimum lift-rate curve(s) can be made for a given field based on tubing size and wellhead-downhole conditions. This minimum lift "type curve" can then be used as an overlay tool to identify potential problem wells.

Well-Performance Monitoring

When a well is completed and placed on production, our focus sometimes shifts to other development projects or operational concerns. Because of today's demanding environment and reduced staffs, individual well performance can go unchecked until an operational or deliverability problem develops. It can be difficult to justify the time needed to assemble and process performance data. In many situations, the procedures and manpower required to collect and maintain the data have disappeared from the functional responsibilities of the organization. One tool the production or reservoir engineer uses to monitor well performance quickly and accurately is the backpressure curve and gas material-balance (p/z vs. cumulative production) plot.

In many cases, the initial source for performance data may be the company's production database, a commercial database, or the well file or data room. This step can be the most time-consuming in the process; once the data are located they must be prepared for analysis.

Data Preparation

The Well Performance Advisor, a personal computer program, is an expert system designed to help the engineer process and maintain a working database for gas-well performance monitoring. There are several data-preparation steps that can be used to help standardize the data and prepare them for plotting and analysis.

1. Wellhead flowing and static pressures should reference the same temperature, normally the average wellhead flowing temperature. One way to accomplish this task is to use an in-house or commercial tubing-design software program to convert wellhead flowing pressure to bottomhole flowing pressure, p_{wf} , at reservoir datum and then back to the wellhead at the select average wellhead flowing temperature. An algorithm based on the Cullender and Smith¹⁸ method performs this calculation very effectively. The process will provide temperature-adjusted values of p_i and p_{wf} .

For low-to-medium-yield gas-condensate reservoirs, we convert the oil condensate to gas equivalent and add this volume to the gas volume. This step determines the full wellstream rate. We use this rate and the effluent gravity to perform tubing calculations. Flowing conditions up to 150 bbl/MMscf have been modeled successfully with this direct solution. Rich gas-condensate reservoirs may require more rigorous methods.

2. We convert the wellhead shut-in pressures to bottomhole at the same reservoir datum and reservoir temperature. These pressures will be used to develop the material-balance curve.

Pressures from the material-balance curve are converted to the wellhead at the same operating wellhead temperature used for the flowing pressures. This technique can dramatically improve the relationship between shut-in and flowing values plotted on the backpressure curve, especially in offshore situations where 100°F-differences are common between flowing and shut-in conditions.

3. We convert the cumulative oil-condensate production to gas equivalent and add it to the cumulative gas production. This step provides a full wellstream cumulative, Gp , to plot against the bottomhole pressure for the material-balance plot.

4. We construct the p/z vs. cumulative production plot using the wellhead shut-in pressures converted to datum, along with any available measured bottomhole shut-in pressures that have been adjusted to datum. We calibrate calculated and measured pressures and use the appropriate (single- or two-phase)^{19,20} gas deviation factor to determine p/z for each point. The complete form of the material-balance equation is defined in Eq. 9. This form of the material-balance equation is suggested as the y-axis parameter vs. cumulative full wellstream production,

$$p/z \left[1 - \bar{c}_e(p)(p_i - p) \right] \dots\dots\dots (9)$$

where $\bar{c}_e(p)$ is the pressure-dependent cumulative effective compressibility term.²¹ $\bar{C}(p)$ can be a single value, calculated as a function of pressure, or assumed negligible and set equal to zero. In the latter case, Eq. 9 will be reduced to p/z .

Material-Balance Curve

The backpressure and material-balance plots now are ready to be generated for a particular well or group of wells in a common reservoir. Analysis as a group is best so that a comparison can be made of similar trends or differences. We also suggest that the well history (tubing, stimulation, and workover), rate/time production curves, and logs be available for reference. The first step is to develop the material-balance trend from available bottomhole and cumulative data. Estimates from mapped or volumetric gas-in-place calculations should be compared with extrapolated trends on the material-balance curve. Some general rules apply:

1. Because all the pressure values have been converted to the same datum, using the same gas analysis, all material-balance curves should start at the same initial, $p/z [1 - \bar{c}_e(p)(p_i - p)]$ value. An exception to this rule would be wells that came on production after depletion of the reservoir.

2. Volumetric depletion behavior plotted with Eq. 7 will be a straight line for single-layer reservoir performance. The straight-line behavior may be a composite of several different straight-line segments.²² Multilayer reservoirs with no crossflow between layers require special analysis.²³

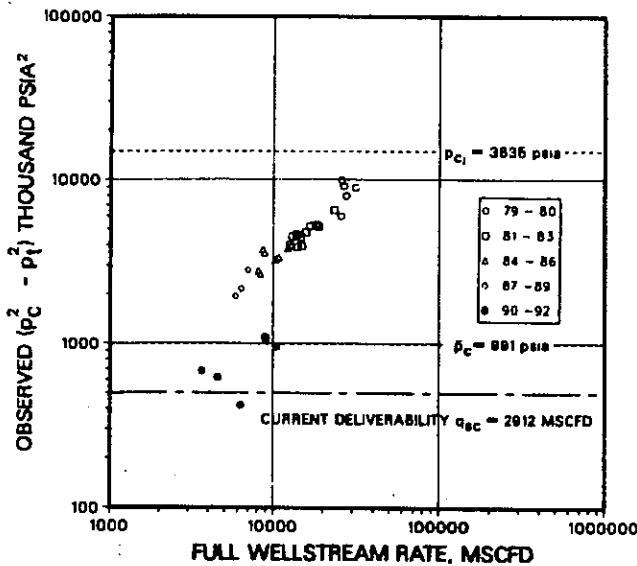


Fig. 1—Wellhead backpressure plot observed data, North Sea example.

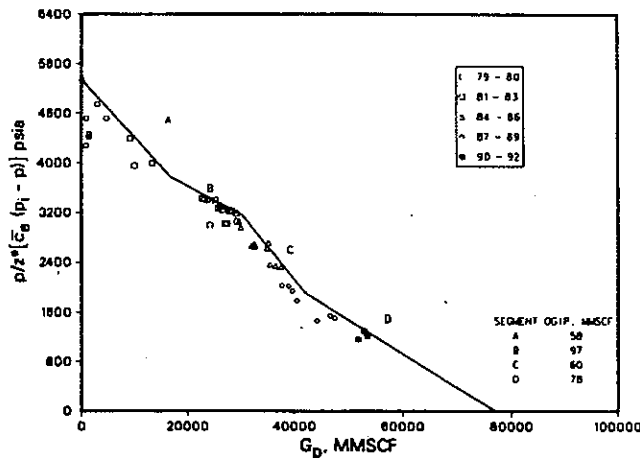


Fig. 2—Pressure vs. cumulative production, North Sea example.

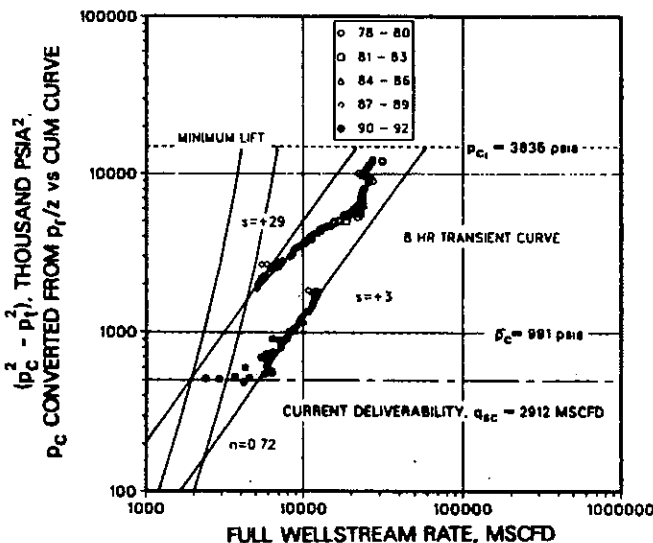


Fig. 3—Wellhead backpressure plot, adjusted and converted points from material balance, North Sea example.

3. The resulting composite material-balance curve, including all wells in the study area, should represent the total gas-in-place supported by geological and reservoir volumetric calculations.

Backpressure Curve

Once the material-balance relationship has been developed, analysis of the wellhead and bottomhole backpressure plots can begin. We generate these plots by several techniques:

1. We determine the static reservoir pressure for each performance point by using the material-balance relationship and the cumulative production at that point. This step provides p_r from the material-balance curve to go with p_{wf} , previously calculated in Step 1 of data preparation.

2. We convert p_r to surface at the same operating wellhead temperature used previously. This conversion will provide the correct p_c to go with the temperature-adjusted p_i , determined earlier.

The reward for performing this step is two-fold. Not only are all p_c values at the same wellhead flowing temperature corresponding directly to the material-balance relationship, but you also gain p_c values that were not available earlier for points that only had a gas rate and flowing pressure.

3. We plot $p_c^2 - p_i^2$ vs. full-wellstream gas rate on 3×3 log-log paper. Delta-pressure squared normally is plotted for most pressure levels, but for high-pressure reservoirs, delta pressure is sometimes required for the wellhead curve.

4. We plot $p_r^2 - p_{wf}^2$ vs. full-wellstream gas rate on log-log paper for reservoir pressures less than 2,500 psi using Eq. 1. For higher pressure reservoirs, use the pseudopressure function for more accurate calculations.

Case Histories

North Sea Example. The first case history concerns well-performance evaluation for a North Sea gas-condensate reservoir. The main pay section is a Paleocene sand at 9,600 ft subsea. The gross thickness of this sand is 700 ft, but owing to interbedded shale and water the net pay averages from 80 to 250 ft. Average porosity is 16.6% and water saturation is 57%. Initial reservoir pressure was 5,315 psia, and the initial GOR was 12,900 (78 bbl/MMscf). Permeability ranges from 3 to 9 md. The wells were drilled and completed during 1976-77, and the field was put on production in early 1978. All wells were completed with 7-in. casing and 4.5-in. tubing. Perforation was performed with $2\frac{1}{8}$ -in. enerjet guns with 4 shots/ft.

Fig. 1 presents the wellhead backpressure plot for a North Sea gas-condensate well. The plot consists of monthly well test points, starting in 1979 and continuing through 1992, where measured static and flowing pressure were available. Well tests were conducted monthly by flowing the well through a test separator for 8 hours after a shut-in. The data plotted are actual reported flowing pressure and associated shut-in static pressure. Without the well history and better definition, Fig. 1 shows little character to quantify performance.

Fig. 2 presents the material-balance curve prepared by using observed wellhead shut-in pressures calibrated to bottomhole measured values. This curve has been determined from a very detailed reservoir analysis, not a trend analysis. The straight-line segments represent changes in the well's drainage area over time. As Fig. 2 illustrates, four major changes occurred, indicated by the original-gas-in-place values for each segment.

The total gas in place of the field was established through geological, reservoir, and performance analysis. Each well was analyzed with the backpressure and material-balance techniques presented in this paper. The permeability level is high enough to develop pseudosteady-state conditions rather quickly. At pseudosteady state, each well in the field drains an area equal to the ratio of its deliverability to the total field deliverability. This relationship was analyzed for each well over their entire production history. The change in this ratio formed a basis to establish each well's proportionate share of the total gas in place.

Fig. 3 is the wellhead backpressure plot for this same well. Each pressure point on this curve is at the same wellhead temperature, and each static pressure comes from the material-balance curve and then is converted to the surface. Many wellhead points that did not have

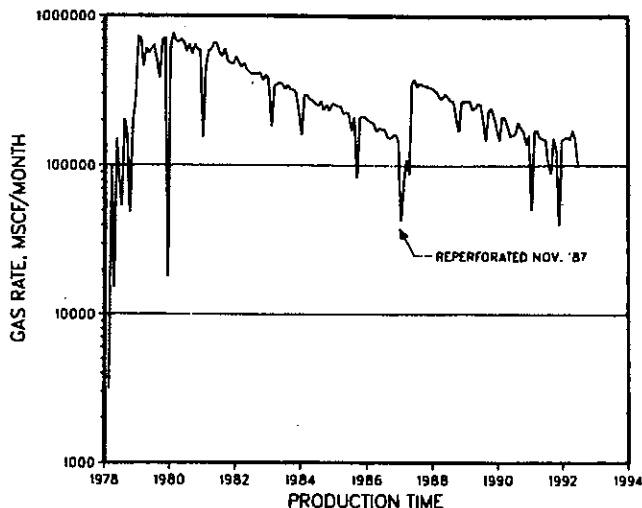


Fig. 4—Gas production vs. time, North Sea example.

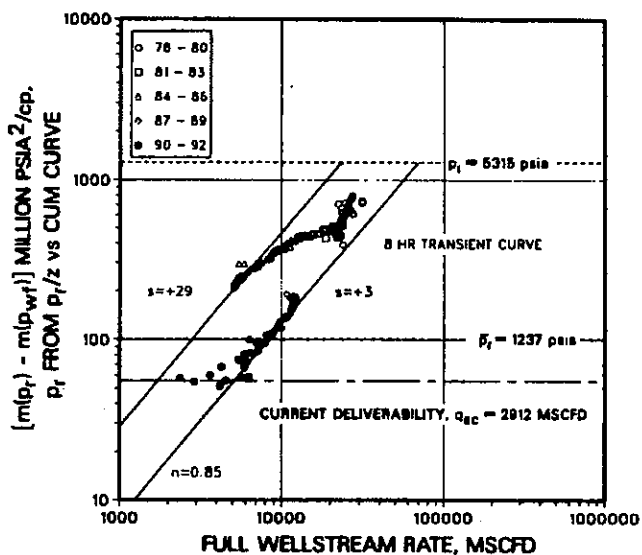


Fig. 5—Bottomhole backpressure plot, calculated backpressure curve, North Sea example.

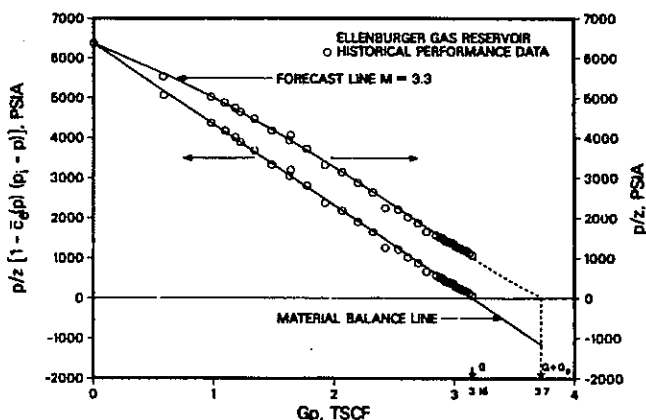


Fig. 6—Pressure vs. cumulative production, Ellenburger gas reservoir.²¹

a corresponding static pressure are available now. Fig. 3 represents 14 years of production performance. An examination of this plot with the well history reveals its characteristics. The movement of the initial performance points to the right (circles), representing the years 1978–80, possibly reflects the well cleaning up. Initial pro-

duction was up and down during 1978–79, and the well did not produce consistently until Feb. 1980. Beginning in 1980 and continuing until late 1987 (diamonds), deliverability slowly deteriorated, possibly the result of fines migration.

In Nov. 1987 the producing interval was reformed at 4 shots/ft. There is a gain in wellhead deliverability, represented by the points that shifted to the right. The straight line through the points is the bottomhole 8-hour transient curve, calculated with Eq. 5 and converted to the surface using the Cullender and Smith method. The line on the left represents a skin effect of +29 before reformation, and the line on the right represents a skin of +3 achieved after reformation. The minimum lift-rate curves for water and condensate are also presented on Fig. 3. The minimum lift curves were generated by using Eq. 7 at wellhead conditions. The curves are used by taking the current wellhead flowing pressure, 780 psia in this case, and squaring this value. At 608 (thousands) on the y axis, we read the minimum rate required to lift water, 3 MMscf/D, and the minimum rate for condensate, 2 MMscf/D. As indicated on Fig. 3, two recent points are slightly below the rate to lift water and have fallen to the left of the established wellhead curve. This well's performance may soon be curtailed because of problems with lift velocity if its deliverability cannot be maintained.

Fig. 4 presents the rate/time history profile. As the plot indicates, it is difficult to identify the reason for the slow change in deliverability during 1980–87. There is an obvious increase in production after the Nov. 1987 reformation. Without the backpressure curve, normal production decline would be the evaluation. All three plots, (backpressure, material-balance, and rate/time), must fit together to describe the reservoir flow characteristics accurately.

Fig. 5 presents the bottomhole backpressure plot. The straight line through the points on the far left was calculated by using Eq. 5 with a time of 8 hours and a pressure-transient well test flow-capacity, kh , of 1,100 md-ft. A skin factor of +29 was required to match the observed points. A high-velocity flow coefficient was determined from the Tessem²⁴ relationship for small-mean-diameter pores. The straight line on the right represents the same reservoir parameters with a skin of +3. Performance since Nov. 1987 has declined at a slower rate. In June 1991, an additional 22-ft interval was perforated. A slight shift to the right is indicated by the circled plus-signs.

In this example, the well's deliverability deteriorated for 7 years, while other wells in the field reduced its initial drainage volume. The well produces in a noncompetitive reservoir environment. Use of the backpressure curve for performance monitoring can identify situations similar to this that are in competitive environments.

Ellenburger Example. This case history describes several wells that produce from the Ellenburger formation. The Ellenburger is a 1,600-ft-thick dry gas reservoir at 13,500 ft with an initial reservoir pressure of 6,675 psia at 200°F. Initial gas composition includes over 28 mol % CO₂. Because of an extensive microfracture system, permeability is high (+75 md), and the wells in the field build up instantaneously. Attempts to conduct bottomhole pressure-transient tests have been difficult because of the short buildup time, wellbore storage effects, and interference from offset wells.

Fig. 6 presents the material-balance relationship for this field.¹² The classic p/z -vs.-cumulative-production plot exhibits concave downward behavior. This is because the rock, water, and CO₂ expansion terms are not accounted for in the simple form of the material-balance equation. When the pressure-dependent cumulative compressibility term, $\bar{c}_g(p)$, was applied to the material-balance relationship, the correct gas-in-place was determined for each well and the field.

Fig. 7 presents the wellhead backpressure plot generated with the techniques presented in this paper for Well 1. The data start in 1966 and continue through 1992. The field came on production in 1954. The data presented in this example come from a commercial database and represent annual state deliverability tests for allowable determination. Note the signature of a well that is tubing limited, wellhead backpressure exponent, n , equal to 0.5. This well has been tubing limited for its entire producing life of 38 years.

TABLE 1—CULLENDER 24-HOUR FLOW DATA

Date	P_r (psia)	P_{wf} (psia)	P_c (psia)	P_i (psia)	Q_{sc} (mscf/d)
Oct. 3, 1944	466.1	345.7	435.2	321.2	9,900
Oct. 14, 1944	468.2	424.9	436.8	395.6	4,440
Dec. 11, 1945	422.7	405.1	394.7	378.1	1,947
Dec. 11, 1945	422.7	357.9	394.7	333.0	5,165

appears across most of the gas fields in the continental U.S. and may be attributed to the gas surplus that resulted in production curtailment from 1976 to 1983. A small pumping unit to remove water was installed in 1978, which could also explain higher surface pressures. This general shape is also characteristic of multilayer reservoir performance with no crossflow between layers,^{22,24} which could be occurring between the Chase Group layers in this well. Measured pressures reflect the pressure of the more depleted, high-permeability layer. Some bottomhole measurements are required to help determine the reservoir parameters that affect the p/z curve and backpressure data for Gas Well No. 1.

Fig. 12 presents the wellhead backpressure plot for Gas Well No. 1 with the calculated 3-, 24-, and 72-hour transient bottomhole curves converted to wellhead. Note on Fig. 12 the position of the minimum lift curve for water relative to the performance points. This well produces up the annulus between 7-in. casing and 2³/₈-in. tubing from an open hole completion at 2,800 ft. Wells in this field do produce water, which is removed by a siphon string or pumping unit.

Developing an analysis of multilayer no-crossflow behavior and its effect on the backpressure curve is not within the scope of this paper. The slope of the backpressure curve will be less than one as differential depletion develops between layers. A main conclusion of previous work²³ is that the measured shut-in pressure values will represent the pressure of the high-permeability layer more closely. Therefore, points on the backpressure curve will be plotted by using pressure close to the high-permeability layer plotted at the total gas rate and flowing pressure of all producing layers. Individual layer pressures and bottomhole deliverability are required to develop the system backpressure curve. Further work is required in this area and on Gas Well No. 1's performance data to determine the component resulting from multilayer no-crossflow performance, performance deterioration, and offset-well interference.

Conclusions

1. The backpressure and material-balance curves are effective tools in monitoring gas-well performance when maintained on a regular basis.
2. Analysis of wellhead and bottomhole performance data are enhanced when pressures are adjusted to a common temperature basis and referenced to the material-balance curve.
3. A method is proposed for displaying the minimum lift and erosional gas rate directly on the wellhead backpressure curve. These

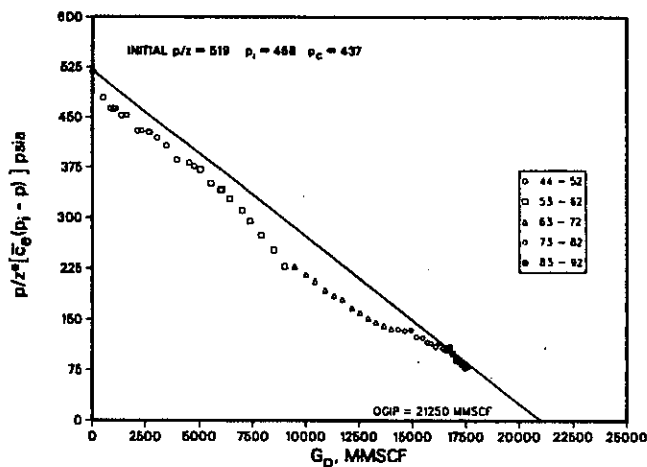


Fig. 11—Pressure vs. cumulative production, Gas Well No. 1.

curves assist the engineer in identifying when liquid loading or erosional rates threaten production optimization. An overlay technique has been identified whereby a minimum lift type curve is generated for an entire field or set of operating conditions.

4. Today's computer workstations provide the engineer with the ability to process and maintain the well-performance data for several hundred wells in an on-line database. Interactive graphical analysis is a suitable environment for data display.

Nomenclature

- A = flow area of conduit, L², ft² [m²]
- C = backpressure coefficient, L³⁻²ⁿt⁴ⁿ/m²ⁿ, Mscf/D-psia² [std m³/d-kPa²]
- \bar{c}_e = cumulative effective compressibility, Lt²/m, 1/psi [1/kPa]
- c_{ti} = total system initial compressibility, Lt²/m, 1/psi [1/kPa]
- D = rate-dependent skin coefficient, (L²/t)⁻¹
- h = formation thickness, L, ft [m]
- h_p = perforated thickness, L, ft [m]
- k = formation permeability, L², md
- L_n = natural log, base e
- m_i = gas viscosity at initial pressure, m/Lt, cp [mPa-s]
- m(p_i) = pseudo pressure at initial reservoir pressure, (MMscf/D)⁻¹ [std m³/d]⁻¹
- m(p_{wf}) = pseudo pressure at bottomhole flowing pressure, psia²/cp
- n = exponent of backpressure curve, dimensionless
- p = pressure, m/Lt², psia [kPa]
- p_i = initial reservoir pressure, m/Lt², psia [kPa]
- p_r = average reservoir pressure, m/Lt², psia [kPa]
- p_{wf} = bottomhole flowing pressure, m/Lt², psia [kPa]
- p_c = wellhead shut-in pressure, m/Lt², psia [kPa]
- p_l = wellhead flowing pressure, m/Lt², psia [kPa]
- q_c = critical gas flow rate, L²/t, MMscf/D [std m³/d]
- q_{sc} = gas flow rate at standard conditions, L²/t, Mscf/D [std m³/d]
- r_w = wellbore radius, L, ft [m]
- s = skin factor, dimensionless
- T = temperature, T, °R
- t_D = dimensionless time
- t = time, t, hours
- v = fluid velocity, LA, q/A, cm³/s-cm²
- v_t = terminal velocity, L/t, ft/sec [m/s]
- z = gas compressibility factor, dimensionless
- ρ_g = gas-phase density, m/L³, lbm/ft³ [kg/m³]
- ρ_L = liquid-phase density, m/L³, lbm/ft³ [kg/cm³]

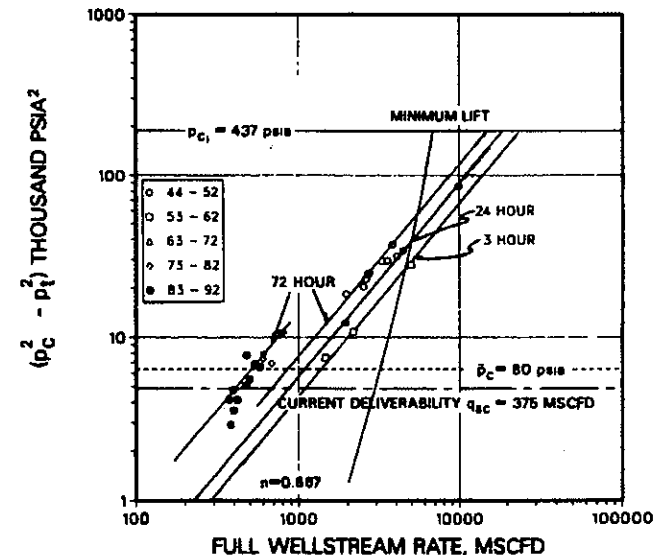


Fig. 12—Wellhead backpressure plot, Gas Well No. 1.

- σ = interfacial tension, m/t², dynes/cm
 γ_g = gas gravity, air = 1.0
 ϕ = porosity, fraction
 μ = gas viscosity, m/Lt, cp [mPa · s]
 β = high-velocity flow coefficient, 1/L, 1/ft [1/m]

Subscripts

- g = gas
 i = initial
 r = reservoir

Acknowledgments

"The development of the method presented was necessarily influenced by the ideas and concepts of others with whom the writer has been privileged to study well performance. To all such persons, grateful acknowledgement is made."—M.H. "Doc" Cullender.² Special thanks to M.J. Fetkovich, to whom I am especially grateful for influencing my ideas and concepts in reservoir engineering. This paper is presented by permission of Phillips Petroleum Co.

References

- Rawlins, E.L. and Shellhardt, M.A.: "Back-Pressure Data on Natural Gas Wells and Their Application to Production Practices," Monograph 7, U.S. Bureau of Mines, Washington, DC (1936).
- Cullender, M.H.: "The Isochronal Performance Method of Determining the Flow Characteristics of Gas Wells," *Trans.*, AIME (1955) 204, 137.
- Smith, R.V.: "Unsteady-State Gas Flow into Gas Wells," *JPT* (Nov. 1961) 1151; *Trans.*, AIME, 222.
- Cornell, D. and Katz, D.L.: "Flow of Gases Through Consolidated Porous Media," *Ind. & Eng. Chem.* (Oct. 1953) 45, 2145.
- Al-Hussainy, R., Ramey, H.J. Jr., and Crawford, P.B.: "The Flow of Real Gases Through Porous Media," *JPT* (May 1966) 642; *Trans.*, AIME, 237.
- Muskat, M.: *The Flow of Homogeneous Fluids Through Porous Media*, Intl. Human Resources Development Corp., Boston (1982) 123.
- Forchheimer, P.: "Wasserbewegung durch Boden," *Zeitz. Ver. Deutsch Ing.*, Berlin (1901) 45, 1781.
- Green, L. and Duwez, P.: "Fluid Flow Through Porous Materials," *J. Appl. Mech.* (March 1951) 18, 39.
- Smith, R.V.: *Practical Natural Gas Engineering*, PennWell Books, PennWell Publishing Co., Tulsa, OK (1983) 95.
- Fetkovich, M.J.: "Multipoint Testing of Gas Wells," SPE Mid Continent Section Continuing Education Course, March 1975, Tulsa, OK.
- Gilbert, W.E.: "Flowing and Gas-Lift Well Performance," *Drill. and Prod. Prac.*, API (July 1963) 769.
- Brown, K.E.: *The Technology of Artificial Lift Methods*, PennWell Books, Tulsa, OK (1984) 2, 322.
- Bizanti, M.S. and Moonesan, A.: "How To Determine Minimum Flow-rate for Liquid Removal," *World Oil* (Sept. 1989) 209, 71.
- Farshad, F.F., LeBlanc, J.L., and Root, P.J.: "A Predictive Model for Analyzing Erosional Velocity and Corrosion Effects Enhances Optimized Production of a Gas Well System," paper SPE 17719 presented at the 1988 SPE Gas Technology Symposium, Dallas, June 13-15.
- Turner, R.G., Hubbard, M.G., and Dukler, A.E.: "Analysis and Prediction of Minimum Flow Rate for the Continuous Removal of Liquids from Gas Wells," *JPT* (Nov. 1969) 1475; *Trans.*, AIME, 246.
- Iiobi, M.I. and Ikoku, C.U.: "Minimum Gas Flow Rate for Continuous Liquid Removal in Gas Wells," paper SPE 10170 presented at the 1981 SPE Annual Technical Conference and Exhibition, San Antonio, Oct. 4-7.
- Coleman, S.B. et al.: "A New Look at Predicting Gas-Well Load-Up," *JPT* (March 1991) 329; *Trans.*, AIME, 291.

- Cullender, M.H. and Smith, R.V.: "Practical Solution of Gas-Flow Equations for Wells and Pipelines with Large Temperature Gradients," *Trans.*, AIME (1956) 207, 281.
- Fussell, D.D.: "Single-Well Performance Predictions for Gas Condensate Reservoirs," paper SPE 4072 presented at the 1972 SPE Annual Technical Conference and Exhibition, San Antonio, Oct. 8-11.
- Vo, D.T., Jones, J.R., and Raghavan, R.: "Performance Predictions for Gas-Condensate Reservoirs," *SPEFE* (Dec. 1989) 576; *Trans.*, AIME, 287.
- Fetkovich, M.J., Reese, D.E., and Whitson, C.H.: "Application of a General Material Balance for High-Pressure Gas Reservoirs," paper SPE 22921 presented at the 1991 SPE Annual Technical Conference and Exhibition, Dallas, Oct. 6-9.
- Stewart, P.R.: "Evaluation of Individual Gas Well Reserves," *SPEFE* (May 1966) 85.
- Fetkovich, M.J. et al.: "Depletion Performance of Layered Reservoirs Without Crossflow," *SPEFE* (Sept. 1990) 310; *Trans.*, AIME, 289.
- Tessem, R.: "High-Velocity Coefficient's Dependence of Rock Properties: A Laboratory Study," PhD dissertation, Norwegian Petroleum Inst., Trondheim (Dec. 1980).
- Golan, M. and Whitson, C.H.: *Well Performance*, Prentice-Hall Inc., Englewood Cliffs, NJ (1991) 223.
- Fetkovich, M.J., Ebbs, D.J., and Voelker, J.J.: "Development of a Multi-layer Model to Evaluate Infill Drilling Potential in the Oklahoma Hugoton Field," *SPEFE* (Aug. 1994) 162.
- Russell, D.G. et al.: "Methods for Predicting Gas Well Performance," *JPT* (Jan. 1966) 99; *Trans.*, AIME, 237.
- Green, W.R.: "Analyzing the Performance of Gas Wells," *JPT* (July 1983) 1378; *Trans.*, AIME, 275.

SI Metric Conversion Factors

bbl × 1.589 873	E - 01 = m ³
cp × 1.0*	E - 03 = Pa · s
dync/cm × 1.0*	E + 00 = mN/m
ft × 3.048*	E - 01 = m
ft ³ × 2.831 685	E - 02 = m ³
°F (°F - 32)/1.8	= °C
in. × 2.54*	E + 00 = cm
psi × 6.894 757	E + 00 = kPa

*Conversion factor is exact.

SPEPF

Thomas S. Thrasher is a senior staff reservoir engineer supervisor in the Research & Services Div. of Corporate Technology at Phillips Petroleum Co. in Bartlesville, OK. Since joining Phillips in 1976, he has worked and conducted training worldwide on pressure-transient analysis and on-site well test supervision, reservoir simulation, hydraulic fracturing, well performance, production forecasting, and reservoir engineering. Thrasher holds a BS degree in petroleum engineering from the U. of Oklahoma. He has held several Bartlesville Section offices and was the 1991-92 Chairman. Thrasher served on the 1987-90 Annual Meeting Technical Program Committee on pressure-transient analysis and since 1993 has been a member of the Electronic Publishing Committee, of which he is the current chairman.

